CERN-TH.6222/91

New Jet Cluster Algorithms: Next-to-leading Order QCD and Hadronization Corrections

S. Bethke
Physikalisches Institut,
University of Heidelberg, Germany,
Z. Kunszt
Theoretical Physics, ETH Institute,
Zurich, Switzerland,
D.E. Soper
Institute of Theoretical Science, University of Oregon,
Eugene, Oregon, USA,
and
W.J. Stirling[1]
TH Division, CERN,
Geneva, Switzerland

Abstract

New algorithms have been proposed as alternatives to the standard JADE-type algorithms for quantifying jet production in e^+e^- annihilation. We study in detail the "Durham" algorithm, based on clustering according to relative transverse momentum, and introduce a new "Geneva" variation which is expected to exhibit similar theoretical properties of exponentiation at small jet resolution. In particular, we calculate the next-to-leading order perturbative corrections to the three-jet rate for the new algorithms, and we study non-perturbative corrections using the JETSET parton-shower Monte Carlo. In each case we compare to the results obtained with the usual JADE-type algorithms. We conclude that the new algorithms exhibit somewhat smaller perturbative corrections compared to the standard algorithms, and that the non-perturbative corrections are of comparable size. Thus the new algorithms appear to be at least as well suited to precision measurements of the strong coupling.

CERN-TH.6222/91
August 1991

[1]Permanent Address: Department of Physics, University of Durham, Durham, England.

1 Introduction

Comparisons of the measured rate of multi-jet events with the predictions of perturbative QCD have emerged as one of the most powerful ways of measuring the strong coupling α_s at e^+e^- colliders like LEP.

The most commonly used methods for defining and reconstructing jets at e^+e^- colliders are based on "successive combination" algorithms, originally introduced by the JADE group [1]. Such algorithms are iterative, beginning with a list of jets that are just the observed particles. (In a perturbative calculation, one begins with a list of partons instead.) At each stage of the iteration, one considers two jets i and j as candidates for combination into a single jet according to the value of a dimensionless "jettiness" variable y_{ij}, which may be, for example,

$$y_{ij} = \frac{2E_iE_j(1-\cos\theta_{ij})}{s} . \tag{1}$$

The pair i,j with the smallest value of y_{ij} is combined first. When two jets are combined the four-momentum of the new jet is determined by a combination formula, which may be, for example,

$$P^\mu = P_i^\mu + P_j^\mu . \tag{2}$$

After this joining, there is a new list of jets. The process continues until every remaining y_{ij} is larger than a preset cutoff, $y_{\rm cut}$. In this way, each event is classified as containing two, three, four ...jets, where the number of jets depends on the cutoff $y_{\rm cut}$ chosen.

We shall call the particular successive combination algorithm based on eqs.(1) and (2) the JADE algorithm. The success of this and similar algorithms is mainly due to the fact that the hadronization of the parton final states can be shown to have, on average, little influence on the jet rates [2, 3]. On the other hand, perturbative corrections are rather sizable. Of particular importance is the three-jet fraction $f_3(y_{\rm cut})$ which is known to next-to-leading order (NLO) [3, 4] and which provides a direct measurement of α_s. One of the main obstacles to reducing the error on α_s obtained this way is the substantial renormalization scale dependence, which indicates that perturbative corrections beyond the order calculated are not yet negligable. There are various ways to improve this situation. One could, in principle, calculate to even higher order in perturbation theory. Unfortunately, with presently available techniques this is not a realistic proposition. One is thus motivated to find new algorithms for defining jets, which would have smaller perturbative corrections while maintaining the insensitivity to hadronization of the original JADE scheme.

A second motivation for modifying the existing algorithm comes from theoretical studies of the small $y_{\rm cut}$ region. As pointed out in [5], the jet fractions defined using the formula for y_{ij} given in eq.(1) do not exhibit the usual Sudakov exponentiation from multiple soft gluon emission, despite having an effective expansion in $\alpha_s \log^2(y_{\rm cut})$.

One can give an intuitive picture of why the definition of y_{ij} given in (1) may cause problems, both for the size of higher order corrections at values of $y_{\rm cut}$ that are not small and for the summation of leading logarithms for $y_{\rm cut} \to 0$. The problem arises from soft gluons that, according to QCD perturbation theory, are copiously radiated from the jets in a hard process. One obtains a picture of events consisting of soft particles plus jets, which contain high energy particles that are nearly collinear with one another. Individual soft particles are not really associated with particular jets, but it may be convenient to associate each soft particle with a jet that is nearby in angle. Now the problem with the definition (1) is that two gluons i,j with $E_i \ll \sqrt{s}$ and $E_j \ll \sqrt{s}$ will have a very small value of y_{ij}, even if their directions are not close. Thus the iterative algorithm will combine the soft gluons with each other first, rather than first trying to combine the soft gluons with the high energy particles. The result can be an "artificial" jet made of soft particles. Since fixed order perturbation theory does not do well with soft particles, this effect may introduce large higher order perturbative corrections. It also has the effect of producing an unnatural partitioning of the multi-parton final state which spoils the exponentiation of logarithms of $y_{\rm cut}$ for $y_{\rm cut} \to 0$ [6].

Dokshitzer [7] has pointed out that a better approach to exponentiation is to cluster according to the minimum relative transverse momentum, k_{Tij} of the parton pair. In practice, this involves replacing eq.(1) by

$$y_{Dij} = \frac{2\,\min(E_i^2, E_j^2)(1-\cos\theta_{ij})}{s} . \tag{3}$$

The numerator here is the same as the transverse momentum squared of the lower energy particle with respect to the direction of the higher energy particle in the small-angle limit. We shall call the successive combination algorithm based on (3) and (2) the "Durham" (D) algorithm.

With the Durham algorithm, we see that a soft gluon will only be combined with another soft gluon, instead of being combined with a high energy parton, if the angle it makes with the other soft gluon is smaller than the angle that it makes with the high energy particle.

Another possibility for the definition of y_{ij} is

$$y_{Gij} = \frac{8}{9}\frac{E_iE_j(1-\cos\theta_{ij})}{(E_i+E_j)^2} . \tag{4}$$

We shall call the successive combination algorithm based on (4) and (2) the "Geneva" (G) algorithm. (The factor 8/9 is provided so that the maximum value of $y_{\rm cut}$ for which three jet events can still be obtained from three partons is $y_{\rm cut} = 1/3$, as it is for the JADE and Durham versions of y_{ij}.)

With the Geneva algorithm, we see that a soft gluon will only be combined with another soft gluon, instead of being combined with a high energy parton, if the angle it makes with the other soft gluon is *much* smaller than the angle that it makes with

the high energy particle. In addition, the Geneva version of y_{ij} has the property that it depends only on the momenta of the particles to be combined, and not on the energy $\sqrt{s}$ of the surrounding event.

The purpose of this paper is to compare the various versions of the JADE algorithm, the new Durham and Geneva algorithms, and also the LUCLUS algorithm [8] that is often used in experimental studies.[2] We address the size of higher order petubative corrections, the size of hadronization corrections, and the possible summation of leading logarithms.

In our comparisons, we will consider not only the JADE algorithm, defined by eqs.(1) and (2), but also the commonly used "E","E0", and "p" variations of this algorithm. In these variations, eq.(1) is replaced by

$$y_{ij} = \frac{(p_i^\mu + p_j^\mu)(p_{i,\mu} + p_{j,\mu})}{s} \quad . \tag{5}$$

This is the same as eq.(1) if jets i and j are massless, but it differs if either of the jets has a non-zero mass. In the E algorithm, one uses eq.(5) along with eq.(2). In the E0 and p algorithms, one uses eq.(5) for y_{ij} but changes the four-momentum combination formula (2) by modifying either the total jet three-momentum ($E0$) or the total jet energy (p) in order to keep the jet massless. In practice, the $E0$ algorithm is the most widely used in α_s measurements. The jet algorithms considered in this paper are summarized in Table 1.

In the following section we review the arguments for modifying the JADE algorithm. We show how the invariant-mass clustering criterion spoils the exponentiation of the large logarithms at small $y_{\rm cut}$, and demonstrate explicitly how this problem is solved – at the leading-logarithm level – by the two new algorithms. In Section 3 we present the results of a numerical calculation of the two, three and four jet fractions to $\mathcal{O}(\alpha_s^2)$. We compare the size of the various higher order corrections, and give simple analytic fits to facilitate the phenomenology. In Section 4 the effects of hadronization on the parton-level calculations is investigated. Using the JETSET Monte Carlo, the jet rates and four-momenta according to the different algorithms are calculated with and without hadronization. In particular, we compare the two new algorithms with the various combination scheme versions of the JADE algorithm ($E, E0, p$) and with the LUCLUS cluster algorithm. Finally, in Section 5, we bring together our conclusions.

2 Leading Logarithms

In this section we examine the exponentiation properties of the various algorithms. This issue was addressed in refs. [5,6], and now a systematic study by Catani, Dokshitzer, Olsson, Turnock, and Webber [9] is underway. It is beyond the scope of this

[2] We do not, however, include the LUCLUS algorithm in our NLO perturbative studies, since this algorithm is not suitable for perturbative calculations.

Algorithm	Resolution	Combination	Remarks
E	$\frac{(p_i+p_j)^2}{s}$	$p_k = p_i + p_j$	Lorentz invariant
JADE	$\frac{2E_iE_j(1-\cos\theta_{ij})}{s}$	$p_k = p_i + p_j$	conserves $\sum E, \sum \vec{p}$
E0	$\frac{(p_i+p_j)^2}{s}$	$E_k = E_i + E_j$; $\vec{p}_k = \frac{E_k}{\lvert\vec{p}_i+\vec{p}_j\rvert}(\vec{p}_i+\vec{p}_j)$	conserves $\sum E$, but violates $\sum \vec{p}$
p	$\frac{(p_i+p_j)^2}{s}$	$\vec{p}_k = \vec{p}_i + \vec{p}_j$; $E_k = \lvert\vec{p}_k\rvert$	conserves $\sum \vec{p}$, but violates $\sum E$
D	$\frac{2\cdot\min(E_i^2,E_j^2)\cdot(1-\cos\theta_{ij})}{s}$	$p_k = p_i + p_j$	conserves $\sum E, \sum \vec{p}$; avoids exp. problems
G	$\frac{8E_iE_j(1-\cos\theta_{ij})}{9(E_i+E_j)^2}$	$p_k = p_i + p_j$	conserves $\sum E, \sum \vec{p}$; avoids exp. problems
LUCLUS	$\frac{2\lvert\vec{p}_i\rvert\cdot\lvert\vec{p}_j\rvert\cdot\sin(\theta_{ij}/2)}{\lvert\vec{p}_i\rvert+\lvert\vec{p}_j\rvert}$	$p_k = p_i + p_j$	conserves $\sum E, \sum \vec{p}$; uncalculable in pert. th.

Table 1. Definition of the resolution measures y_{ij} ($d_{\rm join}$ for LUCLUS) and of combination schemes for various jet algorithms; s is the total center of mass energy or - in experimental implementations - the total visible energy squared, $\vec{p}_i$ denotes a 3-vector and $p_i \equiv (E_i, \vec{p}_i)$ is the corresponding 4-vector.

paper to attempt the detailed calculations necessary to fully establish exponentiation. Rather, we seek to illuminate what we see as the essential physical issue by means of a simple example.

Let us consider an event in which there are two or more hard partons with energies of order $\sqrt{s}$ and with the angles between the hard partons of order 1 (*i.e.* not very small.) We concentrate our attention on two of the hard partons, labelled A and B. Suppose also that there are two soft gluons, labelled 1 and 2. We integrate over the momenta of the soft gluons, and consider the integration region in which gluon 1 is nearly parallel to parton A and gluon 2 is nearly parallel to parton B. In this region, the Lorentz invariant integration measure for the two gluons is approximately

$$\int dE_1^2 \; d\theta_{1A}^2 \; d\phi_{1A} \;\; dE_2^2 \; d\theta_{2B}^2 \; d\phi_{2B} \; . \tag{6}$$

The QCD squared matrix element will contain terms that are singular when gluon 1 is soft and nearly parallel to parton A and gluon 2 is soft and nearly parallel to parton B. Such a term is proportional to

$$|\mathcal{M}|^2 \propto \frac{1}{E_1^2\theta_{1A}^2} \; \frac{1}{E_2^2\theta_{2B}^2} \; . \tag{7}$$

Thus there are four logarithmic divergences in the integration. The divergences can be regulated using dimensional regularization or a simple cutoff, then cancelled against contributions from virtual graphs. One will be left with jet cross sections that contain up to four powers of $\ln(y_{\rm cut})$.

To see how this works, one can change variables to

$$\begin{aligned} \epsilon_1 &= \frac{\ln(\sqrt{s}/E_1)}{\ln(1/y_{\rm cut})} \qquad & \tau_1 &= \frac{\ln(1/\theta_{1A})}{\ln(1/y_{\rm cut})} \\ \epsilon_2 &= \frac{\ln(\sqrt{s}/E_2)}{\ln(1/y_{\rm cut})} \qquad & \tau_2 &= \frac{\ln(1/\theta_{2B})}{\ln(1/y_{\rm cut})} \; . \end{aligned} \tag{8}$$

We also change the jet measure variables y_{ij} to

$$\lambda_{ij} = \frac{\ln(1/y_{ij})}{\ln(1/y_{\rm cut})} \; , \tag{9}$$

so that parton pairs $\{i,j\}$ with the largest values of λ_{ij} are combined first.

With this notation, the contribution to the cross section for partons A and B plus the two gluons to make n jets has the form

$$\ln(1/y_{\rm cut})^4 \int_0^L d\epsilon_1 \int_0^L d\epsilon_2 \int_0^L d\tau_1 \int_0^L d\tau_1 \int d\phi_1 \int d\phi_2 \; \Theta_n \; . \tag{10}$$

Here we regulate the infrared divergence using a simple cutoff L instead of dimensional regularization. Terms in the result that are proportional to L^4, L^3, L^2, and L as

$L \to \infty$ will be cancelled by contributions from graphs in which one or both of the two soft gluons are virtual rather than real. The function Θ_n specifies the n-jet region. It equals 1 when the partons are in an n-jet configuration, as defined by the jet algorithm in use, and equals 0 otherwise. For instance, Θ_4 is 1 when $\max(\lambda_{ij}) < 1$. The expressions for Θ_n for $n < 4$ involve the jet combination formula and are thus more complicated.

Let us now consider how partons are joined to make jets according to the JADE algorithm, using the jet measures y_{ij} from eq.(1) for combining partons. In the integration region that we are considering, the jet measures λ_{ij} are

$$\begin{aligned} \lambda_{1A} &\sim \epsilon_1 + 2\tau_1 \\ \lambda_{2B} &\sim \epsilon_2 + 2\tau_2 \\ \lambda_{12} &\sim \epsilon_1 + \epsilon_2 \; . \end{aligned} \tag{11}$$

(Here we have used $\ln(\sqrt{s}/E_A) \sim \ln(\sqrt{s}/E_B) \sim \ln(1/\theta_{12}) \sim 0$.)

We are now in a position to see the "soft-gluon" problem associated with the JADE jet definition. We see that there is a four-dimensional region in $\epsilon_1, \epsilon_2, \tau_1, \tau_2$ space in which $\lambda_{12} > \lambda_{1A}$ and $\lambda_{12} > \lambda_{2B}$. In this region, the two gluons 1 and 2 form the "best" jet and are joined together to make a jet before either gluon is joined to parton A or B. However, in the contribution to the squared matrix element considered, *there is no singularity corresponding to a (1,2)-jet.* There will be other contributions to the squared QCD matrix element that have $1/\theta_{12}^2$ singularities. One expects these $1/\theta_{12}^2$ terms to yield (1,2) as the best jet with a cross section proportional to $\ln^4(1/y_{\rm cut})$ if a good jet definition is applied. However, in the present case, one may say that the (1,2) jet is artificial in the sense of not corresponding to the matrix element singularities. In reference [6] it is shown that such artificial jets spoil the exponentiation of the leading logarithms, $\ln^4(1/y_{\rm cut})$. We suspect that the artificial jets may hinder the convergence of perturbation theory at finite values of $y_{\rm cut}$ also.

What is the situation for the two new algorithms? Taking the same situation, the jet measures λ_{ij} obtained with the Durham algorithm, eq.(3), are

$$\begin{aligned} \lambda_{1A} &\sim 2\epsilon_1 + 2\tau_1 \\ \lambda_{2B} &\sim 2\epsilon_2 + 2\tau_2 \\ \lambda_{12} &\sim \max[2\epsilon_1, 2\epsilon_2] \; . \end{aligned} \tag{12}$$

We see that λ_{12} is never the largest of the three λ_{ij}'s as long as the τ's are positive. To examine this in a little more detail, let us consider the integration region $\epsilon_1 > \epsilon_2$, so that $\lambda_{12} \sim 2\epsilon_1$. Then for λ_{12} to be, just barely, the largest of the three λ_{ij}'s requires that $\tau_1 \sim 0$. (That is, θ_{1A} is not small.) Thus an artificial jet can be formed, but it "costs" one power of $\ln(1/y_{\rm cut})$ to form it.

With the Geneva algorithm, eq.(4), one finds

$$\lambda_{1A} \sim \epsilon_1 + 2\tau_1$$

$$\begin{aligned} \lambda_{2B} &\sim \epsilon_2 + 2\tau_2 \\ \lambda_{12} &\sim \max[\epsilon_1 - \epsilon_2, \epsilon_2 - \epsilon_1] \,. \end{aligned} \tag{13}$$

We see again that λ_{12} is never the largest of the three λ_{ij}'s. Again taking $\epsilon_1 > \epsilon_2$, we find that $\lambda_{12} \sim \epsilon_1 - \epsilon_2$. Then for λ_{12} to be, just barely, the largest of the three λ_{ij}'s requires that $\tau_1 \sim 0$ and $\epsilon_2 \sim 0$. Thus an "artificial" jet can be formed, but it costs two powers of $\ln(1/y_{\rm cut})$.

Our simple analysis of this section suggests that there should be no problem with summation of the leading logarithms in the new jet algorithms, as discussed for the Durham algorithm in reference [6] for example. It is not clear to us that the situation for subleading logarithms is equally straightforward, although recently it has been claimed [9] that – at least for the Durham algorithm – the first subleading logarithms *can* be treated systematically. The control over leading logarithms obtained with the new jet algorithms will presumably help extend the range for which theoretical calculations can be used to smaller values of y.

3 Jet fractions to $\mathcal{O}(\alpha_s^2)$

The first step with all algorithms is to compute the lowest non-trivial jet fraction, f_3 at $\mathcal{O}(\alpha_s)$, which is obtained by integrating the $q\bar{q}g$ matrix element over the appropriate region of phase space. If d_{ij} denotes one of the "metrics" y_{ij}, y_{Dij}, y_{Gij} defined in eqs.(1,3,4) respectively and $y_{\rm cut}$ the corresponding dimensionless cut-off, then

$$f_3(y_{\rm cut}) = \int_0^1 dx_1 dx_2 \, \theta(d_{ij} - y_{\rm cut}) \, \frac{\alpha_s}{2\pi} \, C_F \, \frac{x_1^2 + x_2^2}{(1-x_1)(1-x_2)} \,, \tag{14}$$

for $i,j = 1,2,3$, where x_1, x_2 are the scaled energy of the quark and antiquark, and $C_F = 4/3$ is a colour factor. It is straightforward to translate the various definitions of the d_{ij} into boundaries in the x_1, x_2 plane [6]. Writing the three-jet fraction as

$$f_3(y) = \frac{\alpha_s}{2\pi} \, A(y) \tag{15}$$

then, with subscripts J, D, G denoting the functions corresponding to the JADE, Durham and Geneva algorithms respectively,

$$\begin{aligned} A_J(y) &= C_F[(3-6y)\log\left(\frac{y}{1-2y}\right) + 2\log^2\left(\frac{y}{1-y}\right) \\ &\quad + \frac{5}{2} - 6y - \frac{9}{2}y^2 + 4\,\mathrm{Li}_2\left(\frac{y}{1-y}\right) - \frac{\pi^2}{3}] \,, \end{aligned} \tag{16}$$

where Li_2 is the usual dilogarithm function, and

$$A_G(y) = A_J\left(\frac{16y}{9(1+y)^2}\right) \,. \tag{17}$$

Note that it is the same function which describes the JADE and Geneva three-jet fraction at $\mathcal{O}(\alpha_s)$. This is because for a three-particle configuration the metrics y_{ij} and y_{Gij} are simply related. An analytic expression for the Durham three-jet fraction has been obtained in [6], but it is rather unwieldy and will not be reproduced here.

It is relatively straightforward to evaluate the $y \to 0$ limit of the $A(y)$:

$$\begin{aligned} A_J(y) &\sim C_F\left[2\log^2 y + 3\log y + \frac{5}{2} - \frac{\pi^2}{3} + \ldots\right] \\ A_G(y) &\sim C_F\left[2\log^2(9y/16) + 3\log(9y/16) + \frac{5}{2} - \frac{\pi^2}{3} + \ldots\right] \\ A_D(y) &\sim C_F\left[\log^2 y + 3\log y + \frac{5}{2} - \frac{\pi^2}{6} + 6\log 2 + \ldots\right] \end{aligned} \tag{18}$$

where ... denotes terms which vanish in the limit $y \to 0$.

The three functions $A(y)$ and their small y behaviour are shown in Fig.1. Note that A_D appears to approach its asymptotic behaviour more slowly, indicating that the leading corrections are $\mathcal{O}(\sqrt{y})$ rather than the $\mathcal{O}(y)$ of A_J and A_G.

When going beyond leading order it is important to specify precisely the jet-fraction definition. For example, one can either normalize the n-jet cross section by the lowest order Born cross section σ_0 – as is natural in theoretical calculations – or by the *total* hadronic cross section $\sigma_{tot} = \sigma_0(1 + \alpha_s/\pi + \ldots)$, as is natural in experimental measurements. The difference between normalizing with σ_0 or with σ_{tot} becomes apparent in the next-to-leading order contributions. In what follows we shall use the definition $f_n = \sigma_n/\sigma_{tot}$, which leads to the constraint $\sum f_n = 1$.

One can write the jet fractions (defined according to some cluster algorithm) in QCD perturbation theory quite generally as

$$\begin{aligned} f_2(y) &= 1 - \left(\frac{\alpha_s(\sqrt{s})}{2\pi}\right) A(y) + \left(\frac{\alpha_s(\sqrt{s})}{2\pi}\right)^2 (2A(y) - B(y) - C(y)) + \ldots \\ f_3(y) &= \left(\frac{\alpha_s(\sqrt{s})}{2\pi}\right) A(y) + \left(\frac{\alpha_s(\sqrt{s})}{2\pi}\right)^2 (B(y) - 2A(y)) + \ldots \\ f_4(y) &= \left(\frac{\alpha_s(\sqrt{s})}{2\pi}\right)^2 C(y) + \ldots \end{aligned} \tag{19}$$

where the coupling constant and coefficients are defined in some appropriate renormalization scheme. In what follows we will use the $\overline{\rm MS}$ scheme. The effect on the jet fractions of evaluating the coupling α_s at an arbitrary renormalization scale μ will be discussed below. Note that in eq.(19) we have used the same definition for the functions A and B as in reference [3], where the jet cross sections were normalized to σ_0.

The B and C terms were first calculated for the JADE algorithm in reference [4]: B receives contributions from final states with real and virtual gluons, while the

leading four-jet contribution C is calculated from the $e^+e^- \to q\bar{q}gg$ and $e^+e^- \to q\bar{q}q\bar{q}$ matrix elements. In reference [3] a procedure was devised for computing the next-to-leading order corrections to *any* three-jet quantity, based on the matrix elements of reference [10]. We use this program to calculate numerically the B and C terms for the new jet algorithms.

In the perturbative calculation of the jet fractions, the original JADE and $E0$ schemes are identical to $\mathcal{O}(\alpha_s^2)$. This is because at most three partons can be combined into a single jet at this order of perturbation theory. Thus the JADE results in this section, labelled with a J subscript, are also valid for the $E0$ algorithm, which is the most widely used algorithm in practice.

The function $B(y)$ defined in eq.(19) is shown in Fig.2 for the three algorithms J, D and G. Fig.3 shows the ratio B/A as a function of y. It is clear that there is a hierarchy of NLO corrections: $G < D < J$. Note that at large y the corrections are roughly independent of y, but that as $y \to 0$ we see clear evidence of the emerging double logarithmic behaviour: in each case the ratio B/A is proportional to $-\log^2 y$ as $y \to 0$. The fact that this happens at larger y for the Geneva algorithm is a direct consequence of the scaling factor introduced in the definition, eq.(4). The same behaviour was also evident in the leading order functions A shown in Fig.1. A more reasonable comparison, therefore, is to compare the next-to-leading order corrections not at the same y value for each algorithm but at an effective y defined such that the three-jet rates are equal at leading order. We therefore define functions $\bar{y}_D(y)$ and $\bar{y}_G(y)$ such that

$$\begin{aligned} A_D(\bar{y}_D(y)) &= A_J(y) \\ A_G(\bar{y}_G(y)) &= A_J(y)\,. \end{aligned} \tag{20}$$

For the Geneva algorithm, it follows from eq.(17) that

$$\bar{y}_G(y) = \frac{8}{9y} - 1 - \frac{4}{9y}\sqrt{4-9y}\,. \tag{21}$$

For the Durham algorithm, $\bar{y}_D$ can be obtained numerically. The two functions $\bar{y}_D(y)$ and $\bar{y}_G(y)$ are shown in Fig.4. Note that by construction $\bar{y}_D(y) = \bar{y}_G(y) = y$ at the kinematic limit $y = 1/3$, where the three-jet rate vanishes in leading order. Fig.3(b) shows the ratio B/A now as a function of the effective y's for the two new algorithms. The behaviour as a function of y is now much more similar – compare Figs.3(a) and (b).

Fig.5(a) shows the four-jet functions $C(y)$ computed numerically at $\mathcal{O}(\alpha_s^2)$ for the three different algorithms. We see again that for a common value of the cluster threshold y, there are more four-jet events for the Geneva algorithm. In fact, the maximum four-jet y value for the Geneva algorithm is 8/27, compared with 1/6 for the JADE and Durham algorithms. Fig.5(b) shows the same quantities plotted as a function of the effective y's. We again see that there are relatively more four-jet events with the Geneva algorithm.

F	Algorithm	y range	k_0	k_1	k_2	k_3	k_4
A	E, E0, p	0.01 - 0.33	3.096	-6.513	3.463	-0.157	0.0134
A	D	0.01 - 0.33	1.725	-3.670	2.149	-0.266	0.0251
A	G	0.02 - 0.33	1.960	-8.057	6.214	-0.744	0.0577
B	E	0.01 - 0.33	51.22	-88.67	0.428	41.64	-6.782
B	E0	0.01 - 0.33	62.63	-91.60	-4.419	40.98	-7.704
B	p	0.01 - 0.33	109.3	-154.6	24.28	30.59	-6.771
B	D	0.01 - 0.33	13.74	-22.63	0.390	9.187	-1.469
B	G	0.02 - 0.33	168.1	-381.0	248.0	-32.41	-4.816
C	E, E0, p	0.01 - 0.12	-47.87	43.13	4.781	-13.37	3.087
C	D	0.01 - 0.10	-17.66	14.84	1.475	-3.995	0.872
C	G	0.02 - 0.24	-100.9	209.3	-140.4	26.90	2.439

Table 2. Parametrisation of the 3- and 4-jet QCD coefficients A, B and C as polynomials $\sum_n k_n \left(\log\frac{1}{y}\right)^n$, for various jet algorithms and combination schemes. The range of validity in y is given for each parametrisation; y values above that range imply that C equals zero.

To facilitate the comparison of the above theoretical predictions with experiment, we have performed simple analytic fits to the functions shown in Figs.2,3(a),5(a). These are of the form

$$F(y) = \sum_{n=0}^{n=4} k_n \left(\log\frac{1}{y}\right)^n\,, \tag{22}$$

for $F = A, B, C$. The coefficients k_n for the JADE ($\equiv E0$), Durham and Geneva algorithms are given in Table 2. Also tabulated, for reference, are the coefficients for the B functions corresponding to the E and p variants of the JADE algorithm.

In the remainder of this section we focus on the three-jet fraction in next-to-leading order for the three algorithms, at $\sqrt{s} = M_Z$. The obvious questions are: how large are the corrections in practice, and how do they depend on the choice of renormalization scale? Fig.6 shows the ratio of the NLO prediction for f_3 – evaluated at renormalization scales $\mu = M_Z\ (= \sqrt{s}), M_Z/2, M_Z/4$ – to the Born level contribution evaluated at scale $\mu = M_Z/2$. Note that the scale dependence for f_3 is introduced in eq.(19) by the replacements

$$\alpha_s(\sqrt{s}) \;\to\; \alpha_s(\mu)$$

$$B(y) \;\rightarrow\; B(y) - A(y)\beta_0 \log\frac{\sqrt{s}}{\mu}\,, \qquad (23)$$

with $\beta_0 = 11 - 2n_f/3$. The predictions are shown as a function of the effective y's, in the region $y_{\rm eff} > 0.05$ where fixed-order perturbation theory should be applicable. We see that the corrections are generally small and rather constant in $y_{\rm eff}$. The emergence of the small-y Sudakov exponentiation is just becoming visible at $y_{\rm eff} = 0.05$. The scale dependence is weaker for the two new algorithms, being correlated with the size of the next-to-leading order function $B(y)$.

Fig.7 shows the μ-dependence at the fixed value of $y_{\rm eff} = 0.1$ for the three algorithms. Also shown (dashed line) is the leading order contribution evaluated at scale μ. The stabilizing effect of the NLO correction is evident. From this figure one can also read off the optimization [11] and fastest-apparent-convergence [12] scales from the position of the maximum and the intersection with the leading-order prediction respectively.

It is encouraging that the new algorithms have somewhat flatter curves than the JADE algorithm. The variation of f_3 over the range $0.1 < \mu/M_Z < 1$ is about 15% for the JADE algorithm but only 8% for the Durham algorithm and 3% for the Geneva algorithm. These numbers can serve as rough lower bounds on the size of the uncalculated $\mathcal{O}(\alpha_s^3)$ corrections. This is because the $\mathcal{O}(\alpha_s^3)$ corrections are guaranteed to cancel the μ dependence of f_3 up to $\mathcal{O}(\alpha_s^4)$, so that these corrections should be *at least* big enough to remove most of the μ dependence seen in Fig.7.

One expects that the value of μ/M_Z where perturbation theory for f_3 works best should not be too far below $\mu/M_Z = 1$, perhaps near $\mu/M_Z = 1/3$ since the three jets tend to share the total energy. Thus one hopes that the curve of f_3 versus μ/M_Z will be flat in just this region. It is thus also encouraging that the region in μ/M_Z in which the curves for the new algorithms are flattest occurs at values of μ/M_Z that are nearer to 1 than for the JADE algorithm.

4 Hadronization Corrections and Jet Resolutions

The question of how useful a cluster algorithm is in practice does not just depend on the size of the higher order perturbative corrections. The non-perturbative process of hadronization also influences the quality and reliability of jet reconstruction in experimental studies. Previous experience with the JADE-type jet algorithms shows that the size of hadronization effects is quite different for the various types of algorithms and is not obviously related to the size of the next-to-leading QCD corrections (see for example [13]).

Hadronization corrections can be studied using QCD-based Monte Carlo event generators, which contain phenomenological models for the transition from quarks and gluons to hadrons. In experimental studies, before the theory can be fitted to the data, either the data (e.g. jet rates) must be corrected for the predicted

hadronization effects, or else the parton-level QCD calculations must be "dressed" with a hadronization model. Systematic uncertainties due to these hadronization corrections are generally small if the correction factors are not too large. In this respect, the JADE-E0 scheme is traditionally favoured because the hadronization corrections to jet production rates are of the order of a few (5-8) percent, in contrast to the larger (about 30%) corrections for the E-scheme [13].

In the following, the influence of hadronization on the different jet algorithms E, E0, p, D and G will be studied. In addition, we also examine a sixth jet algorithm – the LUCLUS jet algorithm [8]. This algorithm is based on an unscaled resolution parameter $d_{\rm join}$ (see Table 1), measured in GeV, and differs in many details from the JADE-type procedure to reconstruct jets. For example, LUCLUS clusters hadrons starting with the fastest particles of the event, and reassigns all particles to the closest jet axis after each combination step. It is for this latter reason that no QCD calculation exists which predicts jet (or parton) rates in a given perturbative order. Because of its good angular and jet energy resolution, LUCLUS is widely used in studies where a direct comparison of data with analytic QCD predictions is not required, and we include it here as a benchmark for the other "QCD-based" algorithms.

For this comparative study we use the JETSET QCD shower plus string hadronization program [8] with parameters optimized to describe global event shapes of hadronic Z^0 decays [14]. The quantities we study are calculated after applying the jet algorithms to the same set of 3000 generated hadronic events. In each case, jets are reconstructed from both the final quarks and gluons at the end of the QCD shower, terminated at a cut-off of $Q_0 = 1$ GeV ("parton level"), and from the particles after hadronization ("hadron level"). For the latter case, all final state particles with lifetimes larger than $3 \cdot 10^{-10}$ s are taken into account, and no simulation of detector acceptance or resolution is applied.

The first quantities we study are simply the relative n-jet production rates, f_n, for n = 2,3,4 and greater or equal to 5. They are shown in Fig.8 as a function of the jet resolution parameter y (or $d_{\rm join}$ in the case of LUCLUS), both for the parton and hadron levels. It is evident that not only are the jet composition and the absolute numbers of n-jet events for given values of y quite different between the algorithms, but also that the size of the hadronization correction, i.e. the difference between hadrons and partons, varies significantly. The absolute hadronization corrections are smallest in the JADE-E0 and in the D scheme, while they are largest for the E and G algorithms. Quantitative comparisons of the value of $y \equiv y_{\rm lim}$ at which the 3-jet rate f_3 at the hadron level is close to 40% (except that for the G scheme the largest possible 3-jet rate is less than 30%) and of the hadronization correction f_3(hadrons) / f_3(partons) at $y \equiv y_{\rm lim}$ are given in the first three rows of Table 3.

To facilitate comparison with the results of the previous section, we show in Fig.9 the size of the hadronization corrections for three algorithms (JADE-E0, D and G) as a function of $y_{\rm eff}$. We see that in each case the corrections are small, and for $y_{\rm eff} > \mathcal{O}(0.05)$ roughly independent of $y_{\rm eff}$. For the Durham algorithm in particular,

the corrections are less than 6% in magnitude in this region.

The net size of hadronization corrections, as dicussed so far, does not entirely reflect the overall influence of hadronization on jet reconstruction. Additional measures to specify the migration of hadronic events from one jet class to another are, for example, the efficiencies and purities of 2-, 3- and 4-jet event reconstruction. Efficiency is defined as the fraction of k-jet events at parton level which is also classified as k-jet event after hadronization, while purity is defined as the fraction of k-jet events at hadron level which originates from genuine k-jet events (at parton level), for identical values of y. The purities and efficiencies which are achieved at $y = y_{\rm lim}$ in our model studies are presented in Table 3. It can be seen that again the E algorithm is worst in both efficiency and purity, while the LUCLUS algorithm appears best, followed by the p algorithm as the most pure and efficient of the "classical", perturbative jet algorithms.

The magnitude of hadronization effects is further demonstrated in two-dimensional correlation plots (Fig.10), where for each hadronic event the value of y_2 at which its classification is changed from a 3-jet to a 2-jet configuration, calculated at both parton and hadron level, is plotted. Vanishing overall hadronization corrections would lead to an event population which is symmetric around the main diagonal $y_2(\text{hadrons}) = y_2(\text{partons})$, while a finite jet resolution causes a certain spread around that diagonal. The largest spread is observed for the E algorithm, which also suffers from a sizable systematic shift away from the main diagonal. The E0 and D algorithms are most symmetric with respect to the diagonal, even at very small values of y_2, while the G and LUCLUS algorithms show large asymmetries in the small y_2 or d_2 regions. The overall width of the two-dimensional distributions is smallest for the LUCLUS, G and p algorithms.

The mean values and the root-mean-square (*rms*) of

$$\Delta y_2 = \frac{y_2(\text{hadrons}) - y_2(\text{partons})}{y_2(\text{hadrons}) + y_2(\text{partons})}$$

are given in rows 10 and 11 of Table 3, for events with $y_2 > y_{\rm lim}$. The mean value of Δy_2 is a measure of the net hadronization correction, while the *rms* value of Δy_2 provides a measure of the finite resolution to reconstruct the parton dynamics of individual events. Since the typical distributions of y_2 differ among algorithms and we want to be insensitive to this difference, we have normalized Δy_2 by $[y_2(\text{hadrons}) + y_2(\text{partons})]$.

Finally, we analyse the jet energy and the angular resolution of 3-jet events identified, at the hadron level, at $y = y_{\rm lim}$. For each of those events, the partons are also combined until a 3-jet configuration is reached, irrespective of the value of y at which this happens. Each parton jet is then uniquely mapped to a hadron jet, starting with the pair which exhibits the smallest angle between the two. We then define

$$\Delta \mathrm{E}_{3-\mathrm{jet}} = \frac{\mathrm{E}_{\mathrm{jet}}(\text{hadron}) - \mathrm{E}_{\mathrm{jet}}(\text{parton})}{\mathrm{E}_{\mathrm{jet}}(\text{hadron}) + \mathrm{E}_{\mathrm{jet}}(\text{parton})}$$

Row	Quantity	E0	E	p	D	G	LUCLUS
1	$y_{\rm lim}$ (or $d_{\rm lim}$)	0.03	0.07	0.02	0.005	0.04	4.5 GeV
2	f_3(hadrons) [%]	40.8	41.2	42.2	39.4	28.2	40.9
3	hadr. correction	0.94	1.30	0.92	0.96	0.85	0.95
4	efficiency (2-jet)	0.92	0.90	0.95	0.91	0.99	0.97
5	efficiency (3-jet)	0.80	0.87	0.81	0.78	0.67	0.83
6	efficiency (4-jet)	0.52	0.79	0.54	0.64	0.40	0.65
7	purity (2-jet)	0.86	0.95	0.84	0.86	0.83	0.86
8	purity (3-jet)	0.85	0.66	0.87	0.80	0.78	0.87
9	purity (4-jet)	0.67	0.31	0.83	0.68	0.67	0.92
10	Δy_2; mean	-0.021	-0.159	0.047	0.109	0.056	0.043
11	Δy_2; *rms*	0.200	0.232	0.148	0.202	0.108	0.055
12	$\Delta\Theta_{3-jet}$; mean	7.3°	10.0°	6.3°	6.3°	5.7°	4.3°
13	$\Delta \mathrm{E}_{3-\mathrm{jet}}$; mean	-0.006	-0.024	0.035	-0.004	0.014	-0.002
14	$\Delta \mathrm{E}_{3-\mathrm{jet}}$; *rms*	0.17	0.21	0.13	0.17	0.15	0.12

Table 3. Comparison of quality features of various jet algorithms, calculated for model events using the JETSET parton shower generator at $\sqrt{s} = M_Z$. The quantities shown in rows 3 to 14 are calculated at a jet resolution $y_{\rm lim}$ ($d_{\rm lim}$ in the case of LUCLUS) which is chosen such that $f_3 \approx 40\%$; for details see the text.

and $\Delta\Theta_{3-jet}$, i.e. the angle between the momentum vectors of a pair of associated parton- and hadron-jets, as quantitative measures of the resolution of jet energies and directions. The mean and *rms* values of the statistical distributions of these quantities are presented in rows 12 to 14 in Table 3. Again we see that the E algorithm shows the worst resolution, while LUCLUS appears to be the best, closely followed by the p algorithm. The E0, D and G algorithms lie between the LUCLUS and E algorithms, with the D algorithm marginally the better of the three.

A word of caution should be added concerning the interpretation of the various numbers and measures given in Table 3. These numbers can only be obtained in Monte Carlo studies where both the final hadrons and partons are known for each event, and the results must therefore be model dependent. We have verified that with the HERWIG QCD shower model [15], which incorporates a different hadronization procedure, the jet finders give similar results compared to what is shown in Table 3

– while the actual numbers can vary slightly between the models, their *relative* sizes are in general the same and the overall conclusions remain unchanged. In addition, our studies do not include effects which arise from the finite acceptance and resolution of a realistic detector. Therefore only the *relative* size of the numbers given in Table 3 should be compared, rather than their *absolute* values.

5 Conclusions

In this paper we have studied several modifications to the standard JADE-type jet-finding algorithms, from the point of view of tests of perturbative QCD. Our motivation was to focus on those algorithms which appear to have a better soft gluon behaviour, which affects the summation of small-y logarithms.

We studied the size of the next-to-leading order perturbative corrections at large y and the size of the hadronization corrections, both of which are important in measuring the strong coupling precisely. In this respect our main conclusions are summarized in Figs.6 and 9. We see that in the region $y_{\rm eff} > \mathcal{O}(0.05)$, both the perturbative and hadronization corrections are well under control for the two new algorithms studied. The Durham algorithm has corrections which are basically everywhere smaller than the "best" of the existing algorithms (E0). In this sense, the Durham algorithm can be considered as providing at least as good a measurement of α_s as the presently used E0 algorithm.

Equally important for future phenomenology is the joining of the fixed-order perturbation series results at large y with the resummed small-y behaviour, to provide a more accurate theoretical expression over a wider range. The effect on the extracted value of α_s and in particular on its uncertainty from scale dependence will be particularly interesting. We have not addressed this question in the present paper, but presumably the results recently claimed for the small-y behaviour of the Durham algorithm in reference [9] are of direct relevance. We would hope that the Geneva algorithm could be analysed in the same way, and would exhibit similar exponentiation properties at small y.

Our study also raises some wider questions about the QCD perturbation theory. When expressed in terms of $y_{\rm eff}$, we have three algorithms (J, D and G) which have identical three-jet rates at leading order, but different next-to-leading order corrections. If one chooses what appears *a priori* to be a sensible value of the scale parameter μ, then the new algorithms have smaller next-to-leading order corrections than the JADE algorithm. Is there any guarantee that an algorithm which has small next-to-leading order corrections has smaller higher order corrections also? Presumably this cannot be answered until such corrections are calculated, but the μ dependence of the next-to-leading order result provides some hints. We have found that the μ dependence for the new algorithms is also smaller than for the JADE algorithm. One could be more confident about the perturbative calculations if one knew exactly what

is controlling the size of the higher order perturbative corrections for the different algorithms. In particular, it is intriguing that the ordering G < D < J observed both for the $\mathcal{O}(\alpha_s^2)$ correction $B(y)$ (including its sign) and for the μ dependence is correlated with the amount of suppression of the "unnatural" jet clustering at small y, as discussed in Section 2. It could well be true that a "good" perturbation theory obtains when the clustering algorithm is well-matched to the underlying singularity properties of the matrix elements.

It is also important to try to understand what feature of the algorithms is determining the size of the hadronization corrections. Here a correlation with the size of the next-to-leading order perturbative corrections is not obvious. Rather than simply study what happens in a particular hadronization model (JETSET, HERWIG, ...) perhaps one could use a simpler model for the way partons merge into hadrons, to see qualitatively how the different corrections arise for the different algorithms.

With these issues of the behaviour of the perturbation series at large y, resummability at small y, and non-perturbative hadronization effects, there is clearly much interesting and important work still to be done in this area of jet physics.

Acknowledgements

Useful discussions with Nick Brown, Stefano Catani, Torbjörn Sjöstrand and Bryan Webber are gratefully acknowledged. Three of us (ZK, DES, WJS) would like to thank the Theory Division at CERN for its kind hospitality.

References

[1] JADE collaboration: S. Bethke *et al.*, Phys. Lett. **213B** (1988) 235.

[2] For a review see, for example, S. Bethke, talk presented at the Workshop on Jets at LEP and HERA, Durham, December 1990, preprint CERN-PPE-91-36 (1991), to be published in Journal of Physics G.

[3] Z. Kunszt and P. Nason, in Z. Kunszt *et al.*, "*Z* Physics at LEP1", CERN Yellow Report 89-08 (1989), Vol.1.

[4] G. Kramer and B. Lampe, Z. Phys. **C34** (1987) 497; erratum *ibid.* **C42** (1989) 504; Fortschr. Phys. **37** (1989) 161.

[5] N. Brown and W.J. Stirling, Phys. Lett. **252B** (1990) 657.

[6] N. Brown and W.J. Stirling, preprint RAL-91-049 (1991).

[7] Yu.L. Dokshitzer, contribution to the Workshop on Jets at LEP and HERA, Durham, December 1990.

[8] T. Sjöstrand, Comp. Phys. Comm. **28** (1983) 227; ibid. **39** (1986) 347; ibid. **43** (1987) 367; M. Bengtsson and T. Sjöstrand, Nucl. Phys. **B289** (1987) 810.

[9] S. Catani, Yu.L. Dokshitzer, M. Olsson, G. Turnock, and B.R. Webber, Cambridge University preprint Cavendish-HEP-91/5 (1991).

[10] R.K. Ellis, D.A. Ross and A.E. Terrano, Nucl. Phys. **B178** (1981) 421.

[11] P.M. Stevenson, Nucl. Phys. **B150** (1979) 357.

[12] G. Grunberg, Phys. Lett. **95B** (1980) 70.

[13] M.Z. Akrawy *et al.*, OPAL Collaboration, Z. Phys. **C49** (1991) 375.

[14] M.Z. Akrawy *et al.*, OPAL collaboration, Z. Phys. **C47** (1990) 505.

[15] G. Marchesini and B.R. Webber, Nucl. Phys. **B310** (1988) 461.

Figure Captions

[1] The functions $A(y)$ which determine the three-jet fractions at leading order, for the JADE, Durham and Geneva algorithms. The analytic small-y behaviours defined in eq.(18) are also shown (dashed lines).

[2] The functions $B(y)$ which determine the three-jet fractions at next-to-leading order, for the JADE (solid line), Durham (dashed line) and Geneva (dotted line) algorithms.

[3] The ratio of next-to-leading to leading coefficients B/A as a function of (a) y and (b) $y_{\rm eff}$, where $y_{\rm eff}$ is defined in the text. The labelling of the curves is the same as in the previous figure.

[4] The functions $y_{\rm eff}(y)$ for the Durham (dashed line) and Geneva (dotted line) algorithms. The JADE algorithm has $y_{\rm eff} = y$, by definition.

[5] The functions C which determine the four-jet fractions at leading order as a function of (a) y and (b) $y_{\rm eff}$, for the JADE (solid line), Durham (dashed line) and Geneva (dotted line) algorithms.

[6] The ratio of the three-jet fractions at next-to-leading and leading order, as a function of $y_{\rm eff}$, for the scale choices $\mu = M_Z$, $M_Z/2$ and $M_Z/4$. A value of $\Lambda^{(5)}_{\overline{\rm MS}} = 120$ MeV is assumed.

[7] The three-jet fractions at next-to-leading order as a function of the renormalization scale μ at $y_{\rm eff} = 0.1$ Note that the Born (leading-order) contribution is the same for the three algorithms. The labelling of the curves is the same as in Fig.2.

[8] Jet rates as a function of the resolution parameter $y_{\rm cut}$ predicted by the JETSET QCD shower model before (partons) and after (hadrons) the hadronization process ($\sqrt{s} = M_Z$).

[9] The ratio f_3(hadrons)/f_3(partons) as a function of $y_{\rm eff}$, as predicted by the JETSET QCD shower model [8], for the three algorithms ($\sqrt{s} = M_Z$).

[10] Distributions of y_2, the value of y at which a hadronic event changes its classification from 3-jet to 2-jet, calculated for JETSET model events before (partons) and after (hadrons) hadronization ($\sqrt{s} = M_Z$).

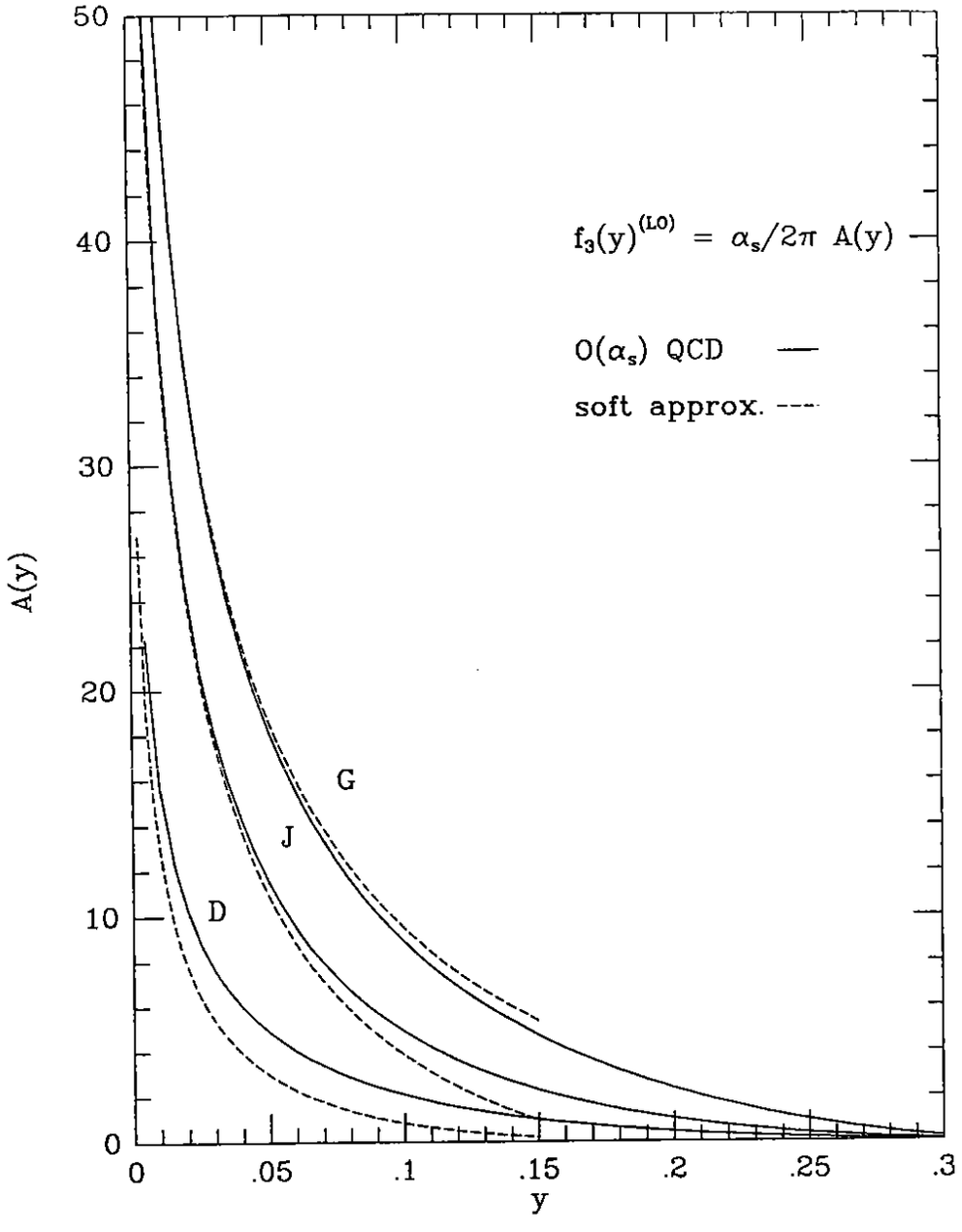
A(y)
y
$f_3(y)^{(LO)} = \alpha_s/2\pi\ A(y)$
$O(\alpha_s)$ QCD
soft approx.
G
J
D
0
10
20
30
40
50
0
.05
.1
.15
.2
.25
.3

Fig. 1

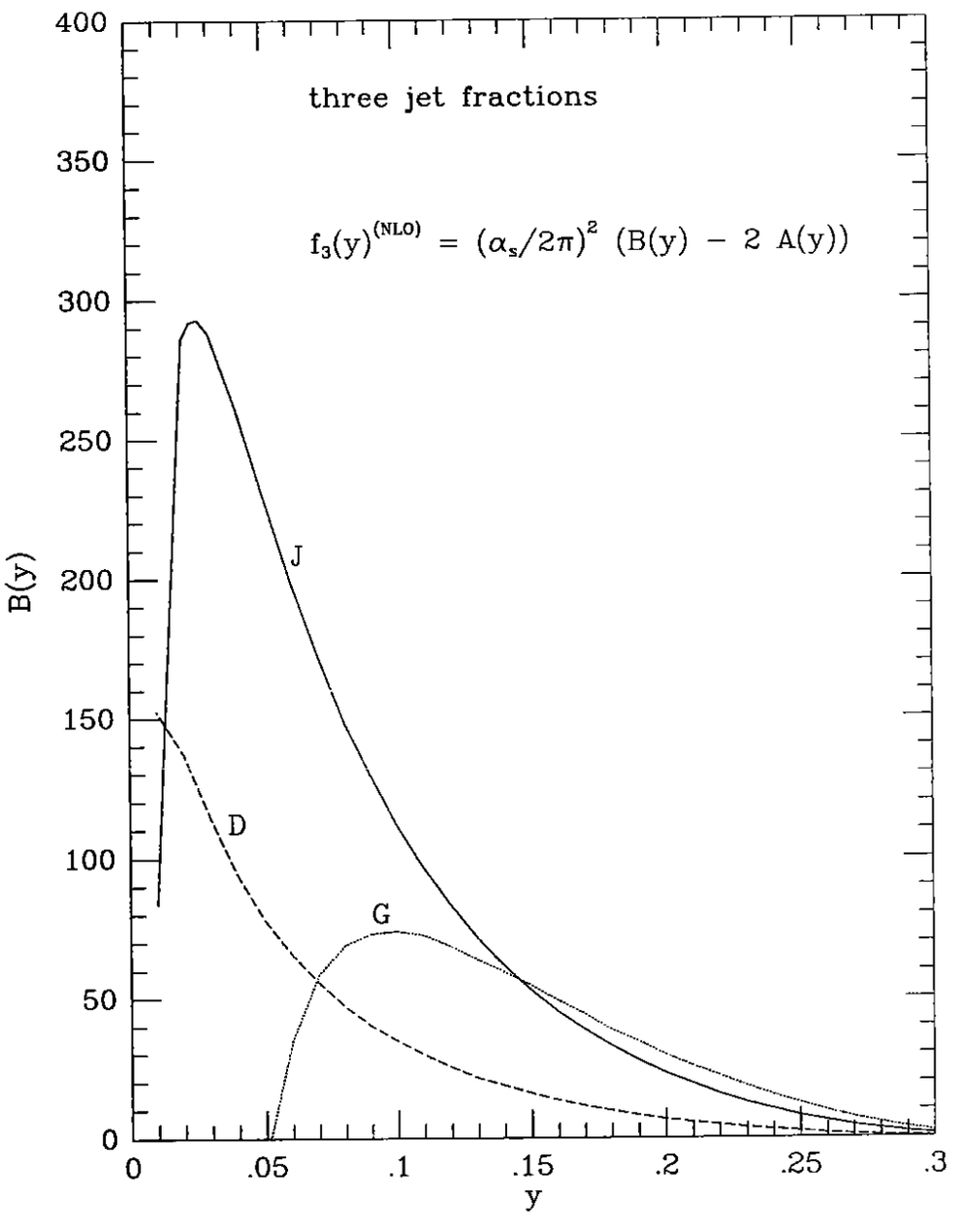
three jet fractions
$f_3(y)^{(NLO)} = (\alpha_s/2\pi)^2\ (B(y) - 2\ A(y))$
B(y)
y
J
D
G
0
50
100
150
200
250
300
350
400
0
.05
.1
.15
.2
.25
.3

Fig. 2

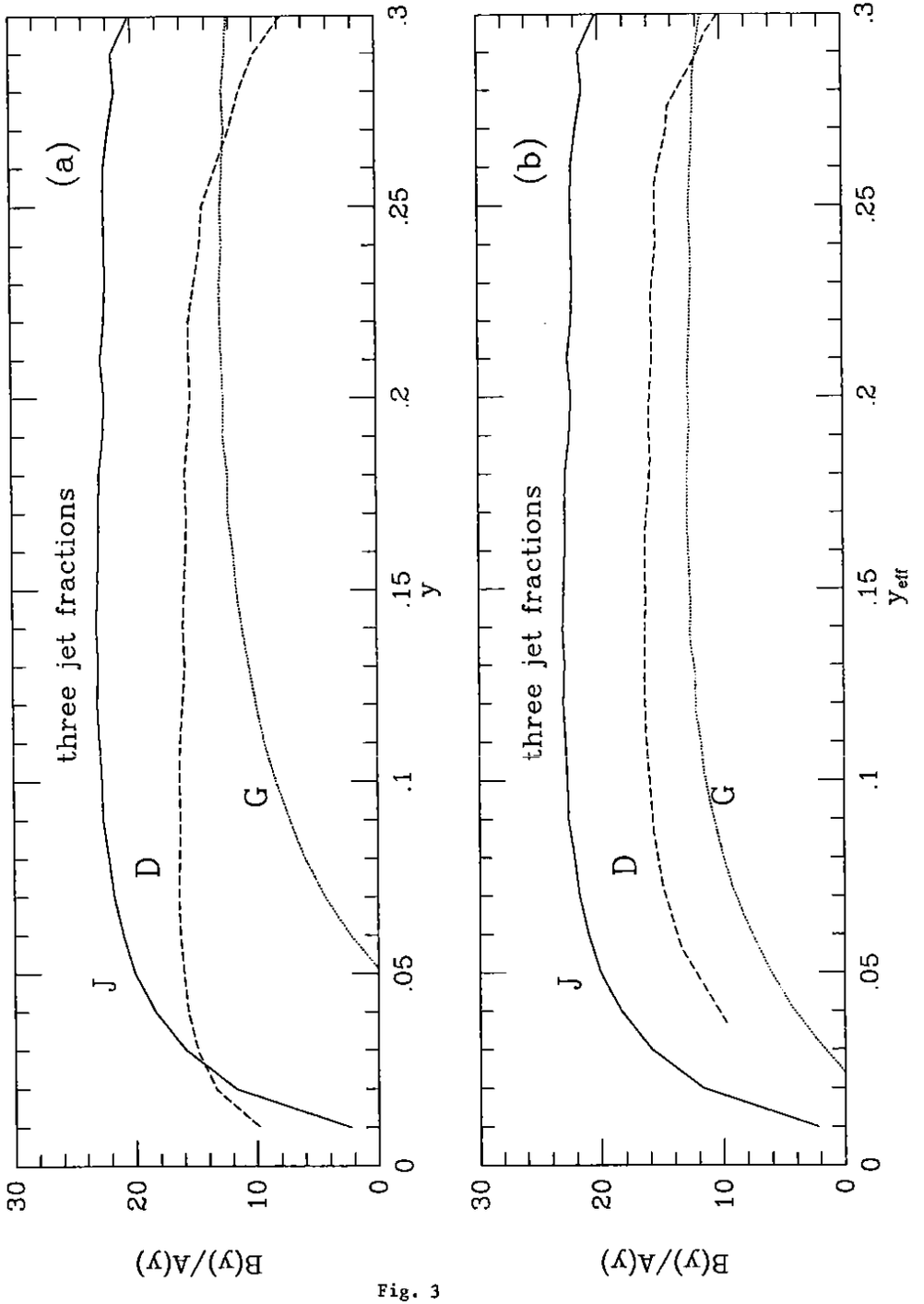
(a)
three jet fractions
J
D
G
B(y)/A(y)
y
(b)
three jet fractions
J
D
G
B(y)/A(y)
y_{eff}

Fig. 3

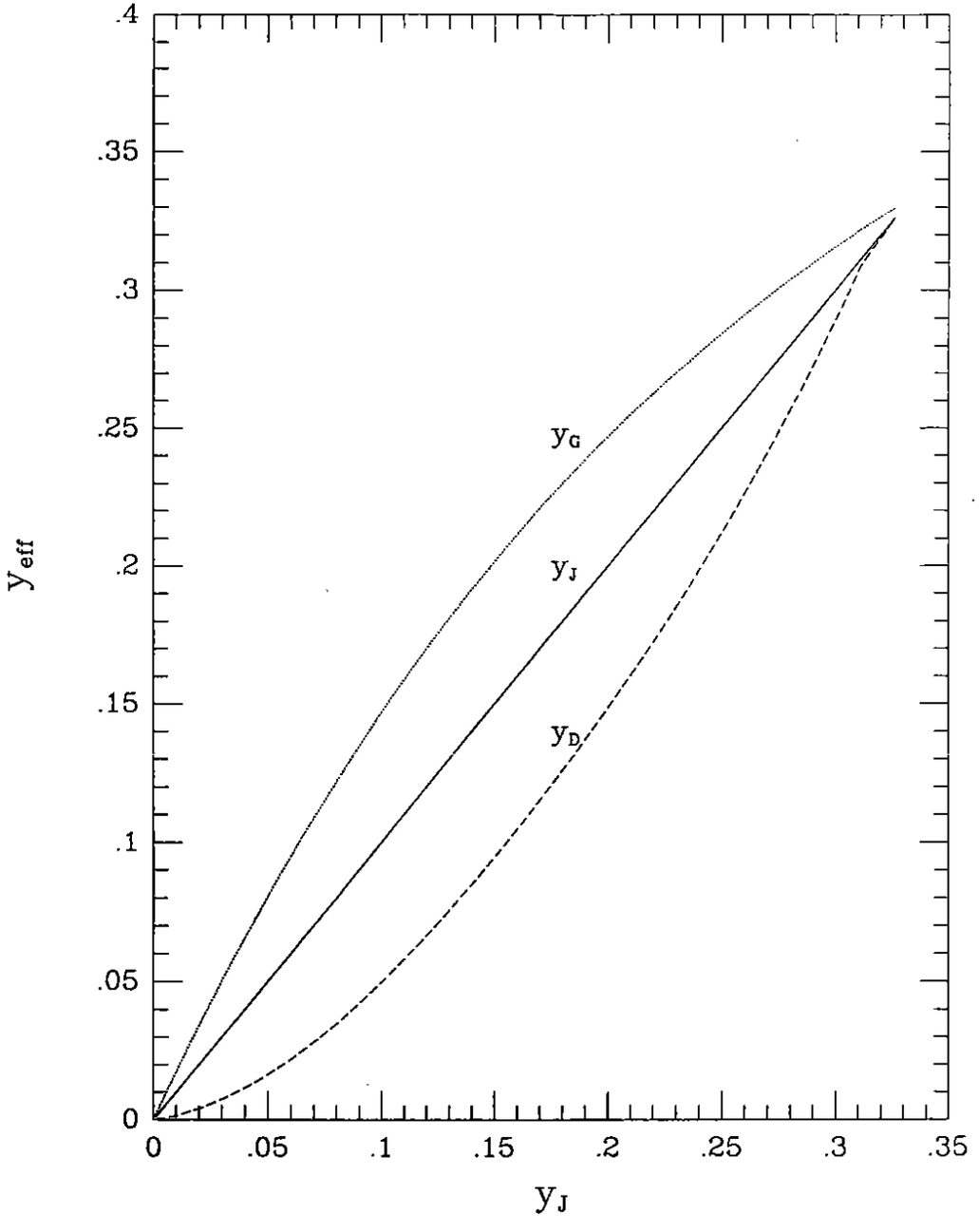
y_{eff}
y_G
y_J
y_D
y_J

Fig. 4

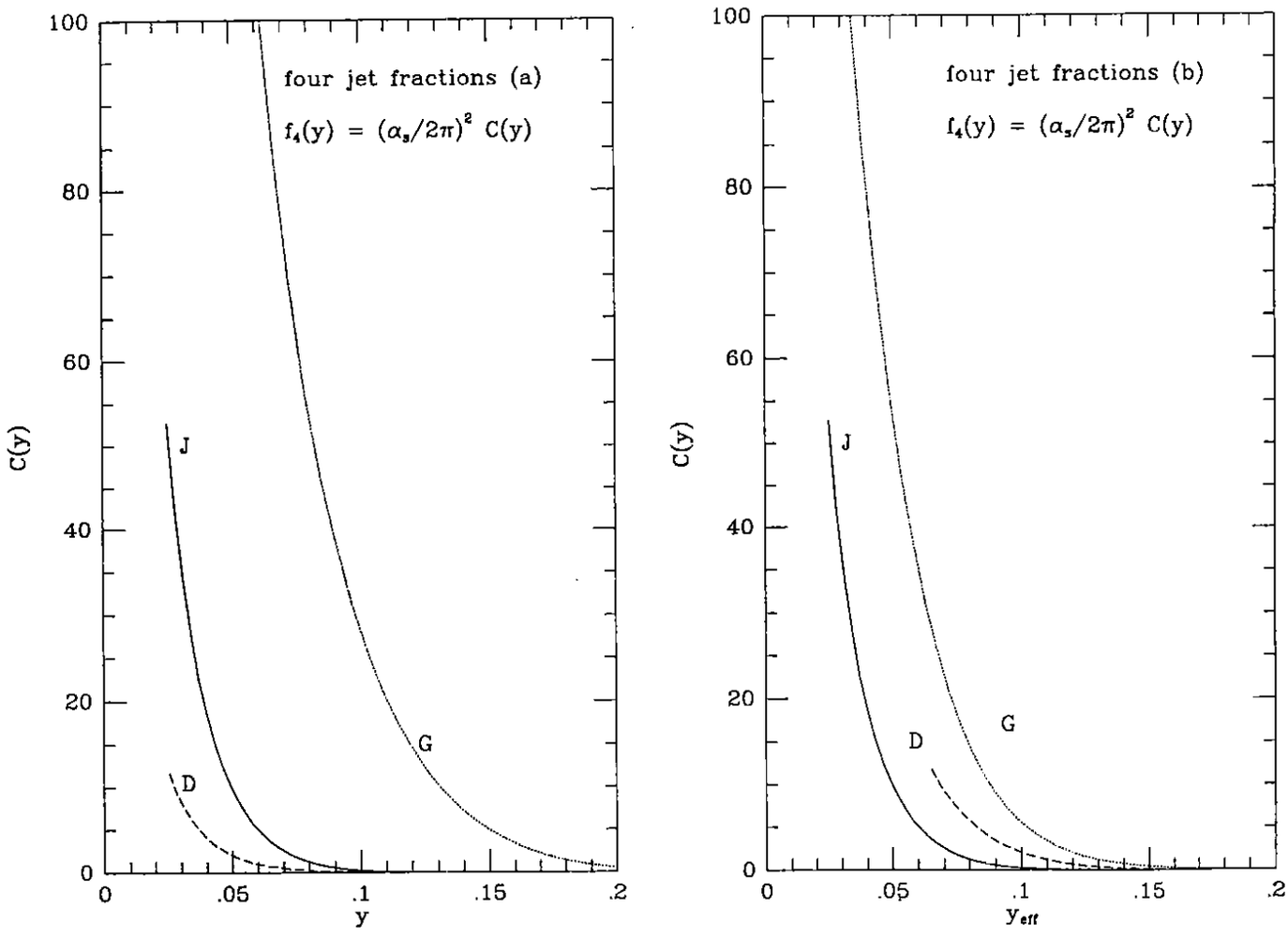
four jet fractions (a)
$f_4(y) = (\alpha_s/2\pi)^2\ C(y)$
C(y)
y
J
D
G
four jet fractions (b)
$f_4(y) = (\alpha_s/2\pi)^2\ C(y)$
C(y)
y_{eff}
J
D
G

Fig. 5

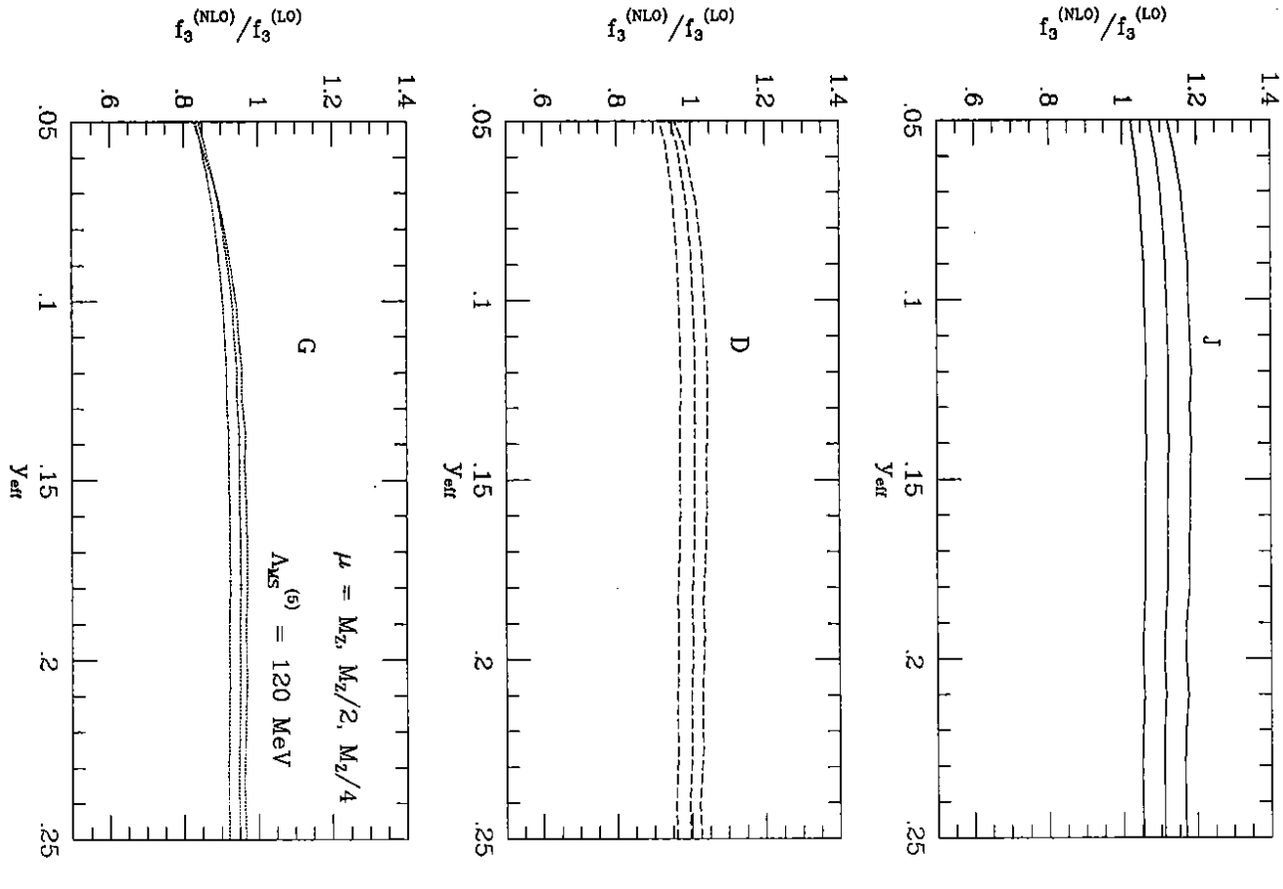
$f_3^{(NLO)}/f_3^{(LO)}$
J
D
G
y_{eff}
$\mu = M_Z,\ M_Z/2,\ M_Z/4$
$\Lambda_{\overline{MS}}^{(5)} = 120$ MeV

Fig. 6

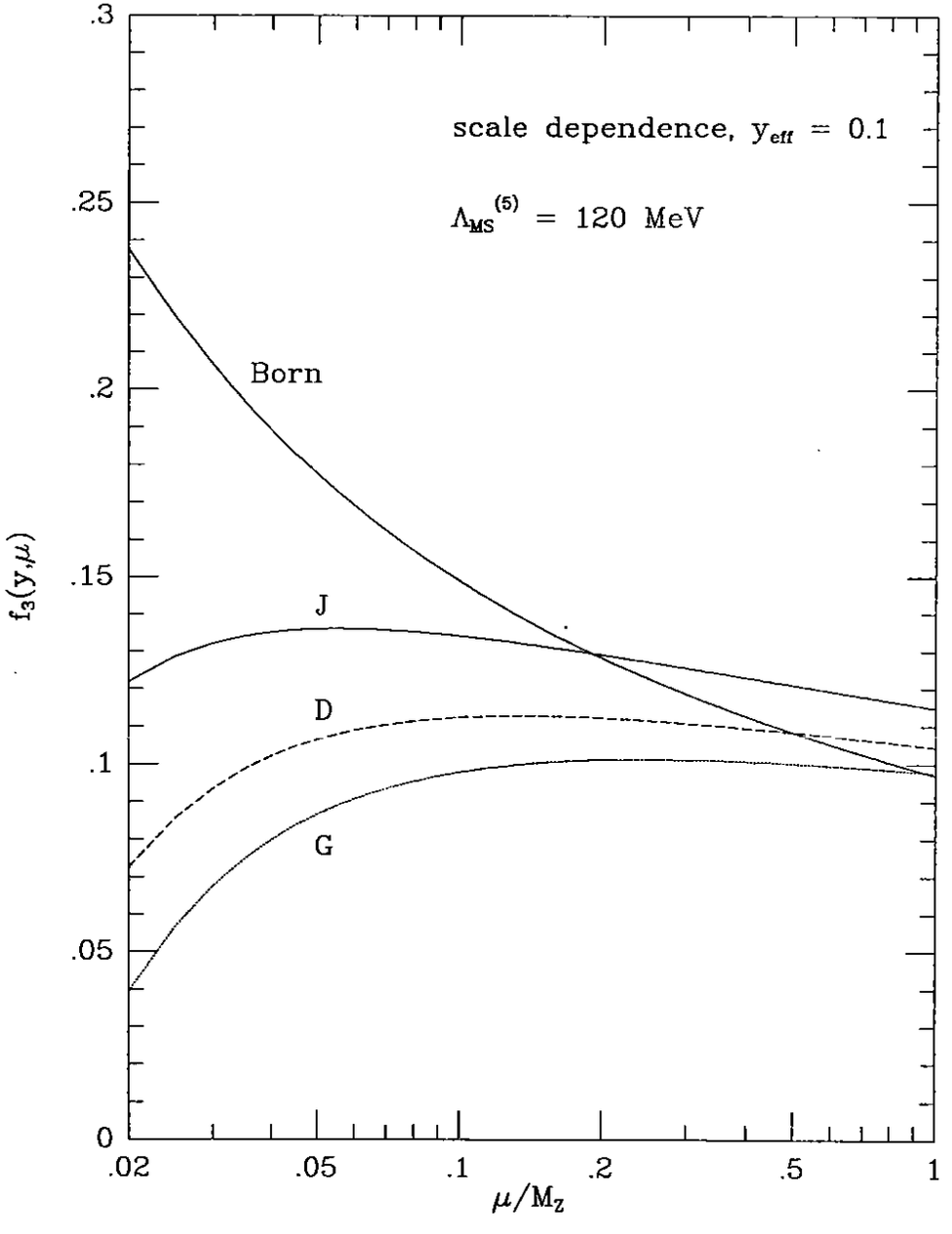
scale dependence, y_{eff} = 0.1
$\Lambda_{MS}^{(5)}$ = 120 MeV
Born
J
D
G
$f_3(y,\mu)$
μ/M_Z
0
.05
.1
.15
.2
.25
.3
.02
.05
.1
.2
.5
1

Fig. 7

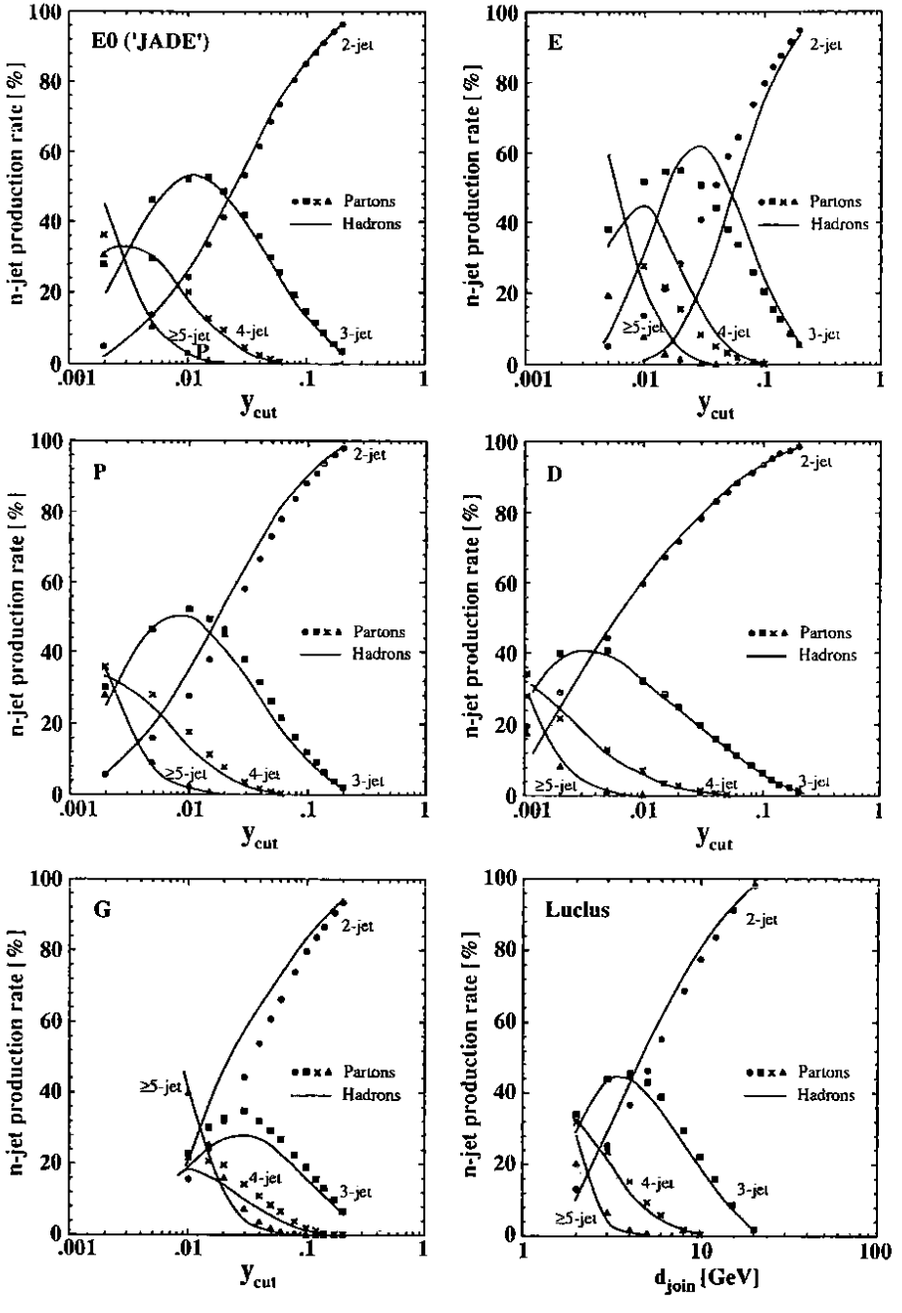
E0 ('JADE')
E
P
D
G
Luclus
2-jet
3-jet
4-jet
≥5-jet
Partons
Hadrons
n-jet production rate [%]
y_{cut}
d_{join} [GeV]

Fig. 8

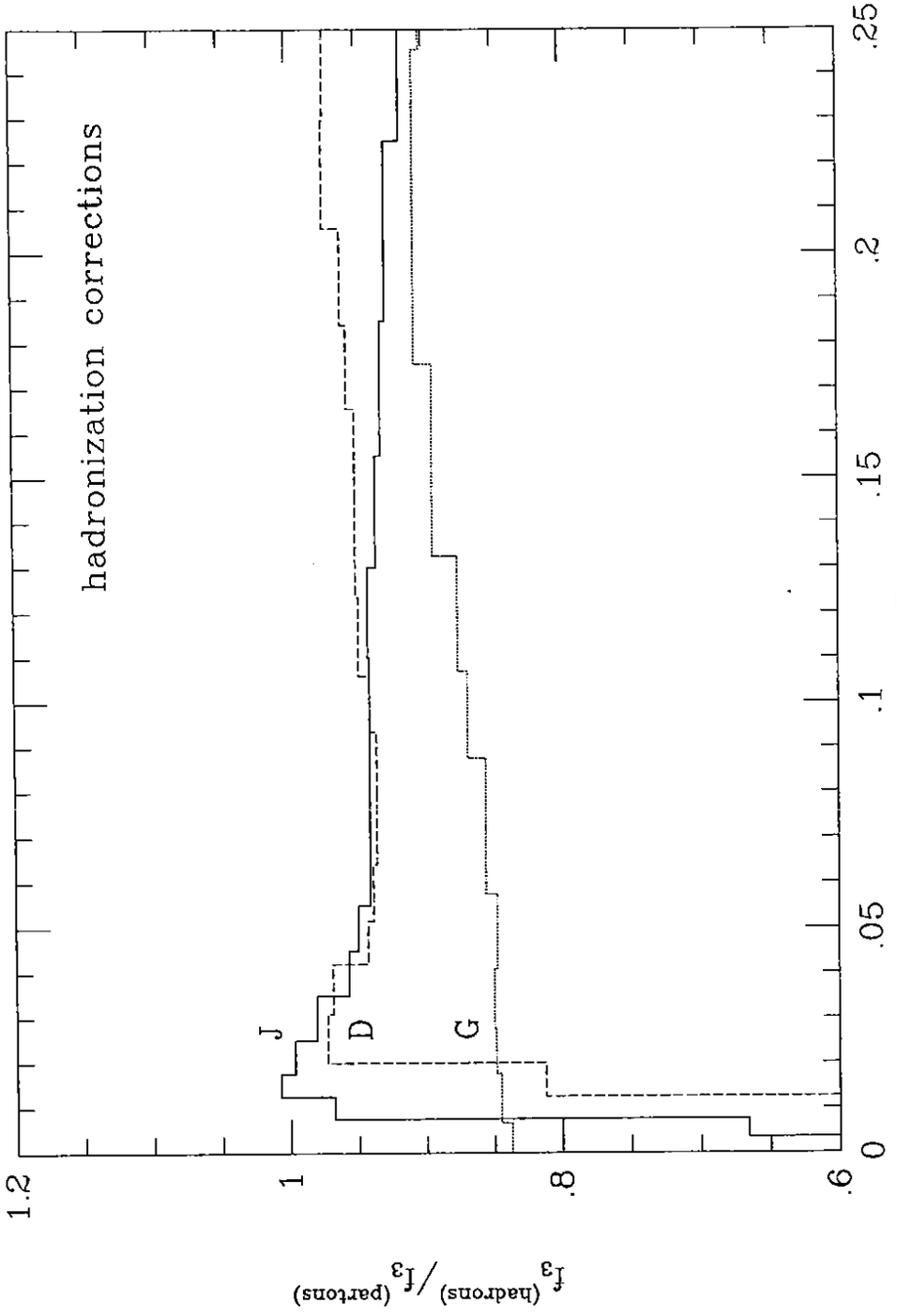

Fig. 9

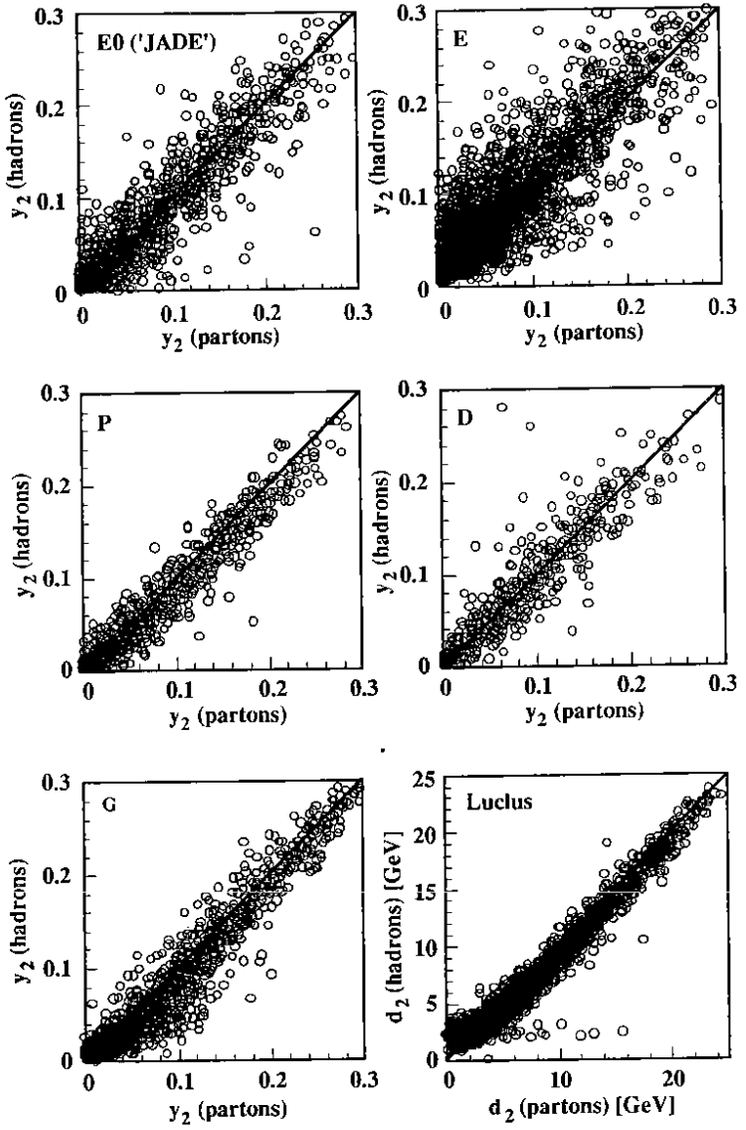

Fig. 10

Imprimé au CERN. Prix : 0.45 Fr.